

Coherent ρ^+ production in neutrino-neon interactions

H. C. Ballagh, H. H. Bingham, T. J. Lawry,* J. Lys, G. R. Lynch, and M. L. Stevenson
Department of Physics and Lawrence Berkeley Laboratory, University of California, Berkeley, California 94720

F. R. Huson,† E. Schmidt, W. Smart, and E. Treadwell
Fermilab, Batavia, Illinois 60510

R. J. Cence, F. A. Harris, M. D. Jones, A. Koide,‡ M. W. Peters, and V. Z. Peterson
Department of Physics, University of Hawaii at Manoa, Honolulu, Hawaii 96822

H. J. Lubatti, K. Moriyasu,§ and E. Wolin**
Visual Techniques Laboratory, Department of Physics, University of Washington, Seattle, Washington 98195

U. Camerini, W. Fry, D. Gee,†† M. Gee,†† R. J. Loveless, and D. D. Reeder
Department of Physics, University of Wisconsin, Madison, Wisconsin 53706

(Received 14 September 1987)

Coherent ρ^+ production on neon nuclei has been observed in charged-current events in a neutrino bubble-chamber experiment. The incident neutrino energy was 10–320 GeV, with a median event energy of 80 GeV. The rate per charged-current event was $(0.28 \pm 0.10)\%$. Comparison was made to vector-meson-dominance predictions; agreement with the overall rate, but disagreement at high neutrino energies and at high Q^2 , was found.

INTRODUCTION

We report here the observation of coherent ρ^+ production by neutrinos on neon, via the reaction

$$\nu\text{Ne} \rightarrow \mu^- \rho^+ \text{Ne}, \quad \rho^+ \rightarrow \pi^+ \pi^0, \quad \pi^0 \rightarrow 2\gamma. \quad (1)$$

The experiment was performed in the Fermilab 15-ft bubble chamber. The neutrino-beam energy range was 10–320 GeV, and the median charged-current-event energy was 80 GeV.

Some years ago several theoretical papers^{1–5} stressed the importance of coherent meson production by neutrinos. These reactions probe the space-time structure of charged and neutral currents and their quantum numbers, and are potential sources of new higher-mass vector and axial-vector mesons. The papers explain the analogy with coherent electroproduction and muoproduction of vector mesons from nuclei, on which there is extensive literature.⁶ The reactions are generally assumed to proceed via the coupling of the weak current to the vector or axial-vector meson, which then scatters diffractively on the target.

Inclusive coherent charged-current reactions on neon have been reported with incident neutrinos⁷ and antineutrinos.⁸ Exclusive coherent production of π^- and ρ^- by antineutrinos on neon^{9,10} (mean incident energy ~ 40 GeV) and of π^+ and π^- by neutrinos and antineutrinos on freon¹¹ (mean incident energy ~ 7 GeV) have also been reported. A preliminary version of the present work is given in Ref. 12.

Coherent neutral-current production of π^0 has been reported by several experiments,^{11,13–16} with mean beam energies up to ~ 31 GeV.

THEORY

The diagram for reaction (1), in the vector-dominance model, is given in Fig. 1. The differential cross section has been given by several authors:^{1–5,17}

$$\frac{d^3\sigma}{dt dQ^2 d\nu} = \frac{G^2 \cos^2 \theta_C}{2\pi^2 E^2 g_\rho^2} \left[\frac{m_{\pi\pi}^2}{Q^2 + m_{\pi\pi}^2} \right]^2 \times \frac{Q^2 F(1 + \epsilon R)}{1 - \epsilon} \frac{d\sigma_\perp}{dt},$$

where t is the square of the four-momentum transfer from the current to the nucleus (we always use the absolute value); Q^2 is the negative of the four-momentum transfer squared; ν is the energy transfer at the lepton vertex; G is the Fermi coupling constant; θ_C is the Cabibbo angle; g_ρ is the current- ρ -meson coupling constant; E is the neutrino energy; F is a flux factor; $m_{\pi\pi}$ is the $\pi\pi$ effective mass; R is the ratio of $d\sigma_L/dt$ to $d\sigma_\perp/dt$, the ρ meson-nucleus differential cross sections for incident meson polarized longitudinally and transversely, respectively; and ϵ is given by

$$\epsilon = \frac{4E(E - \nu) - Q^2}{4E(E - \nu) + Q^2 + 2\nu^2}.$$

The above differential-cross-section formula contains the “standard” Q dependence—the ρ -meson propagator term—of the vector-dominance model. Some relevant discussion, and possible modifications suggested by some electroproduction data, can be found in Ref. 3.

We have used the above formula to make calculations to compare with the experimental results. In our calcula-

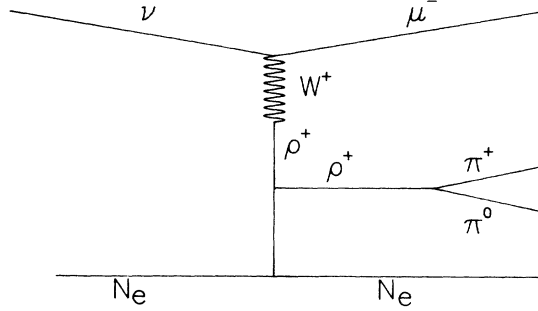


FIG. 1. Vector-meson-dominance diagram for reaction (1).

tions, we take $g^2 g_\rho^2 = 2.1 \times 4\pi$ and $F = \nu$.

We use the optical theorem to write^{8,18}

$$d\sigma_1/dt = \frac{A^2}{16\pi} \sigma_{\text{tot}}^2(\rho^+ N) e^{-bt} F_{\text{abs}},$$

where A is the atomic number of neon and $\sigma_{\text{tot}}(\rho^+ N)$ is the total ρ^+ -nucleon cross section, which we take as 26 mb. We take $b = 79 \text{ GeV}^{-2}$ corresponding to a neon nucleus radius of 3.04 F, and $F_{\text{abs}} = 0.46$ corresponding to an inelastic ρ^+ -nucleon cross section of 20 mb. The factor F_{abs} accounts for reinteractions inside the target nucleus.¹⁸ We set the ratio R to zero at all Q^2 ; at $Q^2 = 0$ gauge invariance requires $R = 0$ (Ref. 3). Some electroproduction and muoproduction experiments have extracted values of R at Q^2 values up to 3 GeV^2 but no clear picture emerges (see Fig. 19 of Ref. 19 and Fig. 15 of Ref. 20). For $m_{\pi\pi}$ we assume a distribution given by a p -wave relativistic Breit-Wigner times a "skew factor" of $m_{\pi\pi}/m_\rho$, as in Ref. 19 (simply setting $m_{\pi\pi} = m_\rho$ reduces the integrated cross section by 11% and makes only small changes in variable distributions).

After changing to the variable $y = \nu/E$, the resulting cross section for neon nuclei is (units cm and GeV)

$$\frac{d^3\sigma}{dt dQ^2 dy} = 166 \times 10^{-38} \left[\frac{m_{\pi\pi}^2}{Q^2 + m_{\pi\pi}^2} \right]^2 \frac{Q^2 y}{1 - \epsilon} e^{-bt}.$$

The dominant factor here is the exponential in t . For our E spectrum this formula predicts that 96% of coherent ρ mesons will have $t < 0.05 \text{ GeV}^2$. Correlated with t is the variable $x = Q^2/(2M\nu)$, where M is the nucleon mass (note not the nucleus mass); the formula predicts that 90% of the events will have $x < 0.10$.

The predicted integrated cross section, as a fraction of the total charged-current cross section, is 0.15% at a neutrino energy of 10 GeV, rises to a maximum of 0.31% at 50 GeV, and slowly falls to 0.20% at 300 GeV. Within the model, uncertainty in the rate arises from uncertainty in the ρ meson-nucleon cross section, in the model for F_{abs} , in the exponential factor b . Also, a nonzero value for the ratio R would increase the rate, while taking the current- ρ -meson coupling constant to be $2.6 \times 4\pi$ (as in Refs. 3, 5, and 10) would decrease the rate.

The decay-angular distribution of the ρ meson can be described by the three angles θ , ϕ , and Φ . Here, θ and ϕ are the helicity frame polar and azimuthal angles of the π^+ in the ρ -meson rest frame, and Φ is the angle between

the lepton plane and the hadron plane (see Refs. 5, 19, and 21). Reference 5 gives general expressions for the decay angular distributions. If we assume s -channel helicity conservation (and natural-parity exchange), the distribution becomes

$$W(\cos\theta, \phi, \Phi) = \sin^2\theta(1 + \epsilon \cos 2\psi) + 2\epsilon R \cos^2\theta \\ - [2\epsilon(1 + \epsilon)R]^{1/2} \cos\delta \sin 2\theta \cos\psi \\ + [2\epsilon(1 - \epsilon)R]^{1/2} \sin\delta \sin 2\theta \sin\psi,$$

where $\psi = \phi - \Phi$ and δ is the phase difference between the longitudinal and transverse amplitudes.

If again we take $R = 0$, only the first term remains, and if $\epsilon \approx 1$ (as is the case for $y < 0.5$) we get a familiar $\sin^2\theta \cos^2\psi$ distribution.

EXPERIMENT DETAILS

Details of the experiment have been reported previously.²² The Fermilab 15-ft bubble chamber filled with a neon-hydrogen mixture (47% atomic neon, radiation length 53 cm) was exposed to a quadrupole triplet neutrino beam produced by 400-GeV protons. A two-plane external muon identifier (EMI) was used for muon identification. 8485 neutrino charged-current events were fully measured, each event had an identified μ^- with energy $E_\mu > 4 \text{ GeV}$. The measurement included all primary charged tracks, all visible neutral-hadron decays, and all possibly primary γ rays that converted into e^+e^- pairs within 110 cm of the primary vertex. Short tracks, generally stopping protons, were measured if their range in the bubble chamber was $> 1 \text{ cm}$, corresponding to momenta $> 200 \text{ MeV}/c$ for protons. After measurement, a γ ray was selected as primary if it (a) pointed to the primary vertex, within errors, and (b) was not consistent with being bremsstrahlung from a measured e^+ or e^- . Also, a track was identified as a proton only if it stopped in the bubble chamber, possibly after a scatter, and its momentum from range was consistent with that from curvature (all identified protons had momenta $< 1000 \text{ MeV}/c$).

COHERENT-EVENT SIGNAL

An initial sample of events was selected by requiring (a) one and only one positive hadron that was not an identified proton (i.e., number of positive hadrons minus number of identified protons equal to unity), (b) no negative hadrons, (c) no primary vees, and (d) exactly two primary gammas. To avoid large errors, fractional momentum errors of < 0.30 for the μ^- and < 0.60 for the positive hadron were also required. No requirement was placed on the number of identified protons; events with no such protons were candidates for reaction (1), while those with protons were candidates for a comparable background sample of nuclear breakup events.

The γ - γ mass distribution from the 76 events selected shows a clear peak at the π^0 mass (Fig. 2). We now select as π^0 events those with a γ - γ mass in the range 100–155 MeV. The $\pi^+\gamma\gamma$ effective mass for the remaining 44 events (we assume the positive hadron is a pion) shows a

clear ρ^+ peak and very little background (Fig. 3). Removing the 3 events with mass > 1200 MeV leaves 41 events which we take to be $\mu^-\rho^+$ events. Of these events, 23 have no identified primary proton and so are candidates for reaction (1).

To proceed to look for coherent events, we look at the four-momentum transfer t . If we assume that an event is coherent, with recoil kinetic energy T_{Ne} of the neon nucleus, then we have²³

$$t = P_1^2 + T_1^2 + 2T_1 T_{\text{Ne}}, \quad (2)$$

where $T_1 = E_\mu - P_{\mu L} + E_\rho - P_{\rho L}$ and hence

$$t = \frac{P_1^2 + T_1^2}{1 - T_1/m_{\text{Ne}}},$$

where P_1 is the magnitude of the observed transverse (to the neutrino direction) momentum imbalance, $P_{\mu L}$ and $P_{\rho L}$ are longitudinal momenta of the μ^- and ρ^+ , respectively, and we again ignore an overall negative sign.

The t distribution for the 23 candidates with no identified proton shows a peak at very small values [Fig. 4(a)]; 11 events have $t < 0.1 \text{ GeV}^2$. In contrast, for the 18 events with identified protons, when we calculate t with neglect of the protons we find just 1 event at $t < 0.1 \text{ GeV}^2$ [Fig. 4(b)]. We attribute the peak in Fig. 4(a) to reaction (1).

To estimate the background of noncoherent events at $t < 0.1 \text{ GeV}^2$ in Fig. 4(a), we suppose that there is a total of three contributing processes: (i) coherent events, essentially all at $t < 0.1 \text{ GeV}^2$, (ii) a background of incoherent diffractive events on quasifree nucleons in the nucleus, and (iii) a background of ‘‘accidental’’ events—events with missing neutrals and hence for which the calculated value of t has little correlation with the actual momentum transfer involved. We now calculate the

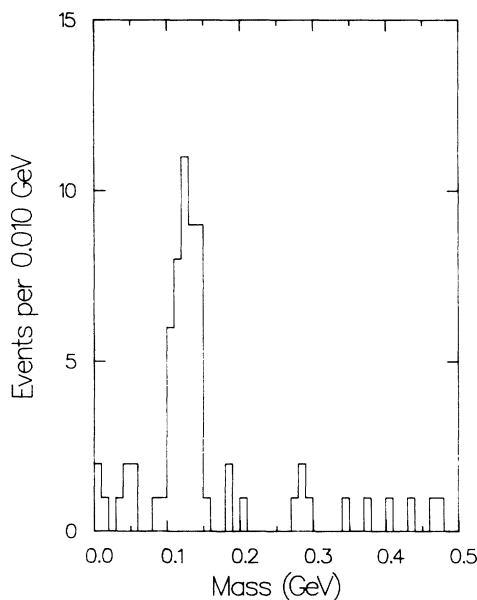


FIG. 2. $\gamma\text{-}\gamma$ mass for selected events—those with a μ^- , just one positive (nonproton) hadron, no negative hadron, exactly two primary gammas, etc. (see text).

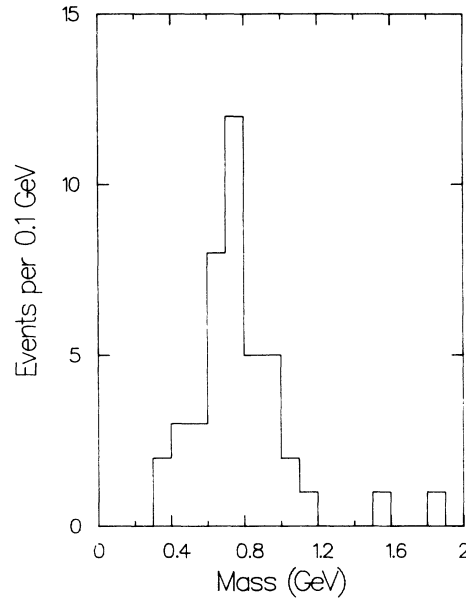


FIG. 3. $\pi^+\text{-}\gamma\text{-}\gamma$ mass for the selected events with $\gamma\text{-}\gamma$ mass in the range 100–155 MeV.

background under two extreme assumptions. First, we assume that there are no incoherent diffractive events. Then, assuming that the t distribution for accidental events is independent of the presence of identified protons, the 1 out of 18 events in Fig. 4(b) with $t < 0.1 \text{ GeV}^2$ and the 12 events in Fig. 4(a) with $t > 0.1 \text{ GeV}^2$ imply 0.7 ± 0.7 accidental events in Fig. 4(a) with $t < 0.1 \text{ GeV}^2$. Second, we assume that there are no accidental events with $t < 0.5 \text{ GeV}^2$, so we are maximizing the number of incoherent diffractive events. Then we use a Monte Carlo model to predict relevant properties of incoherent diffractive events. The Monte Carlo model assumed a vector-dominance model with an e^{-7t} dependence typical of nucleon diffractive processes,²⁰ included Fermi motion

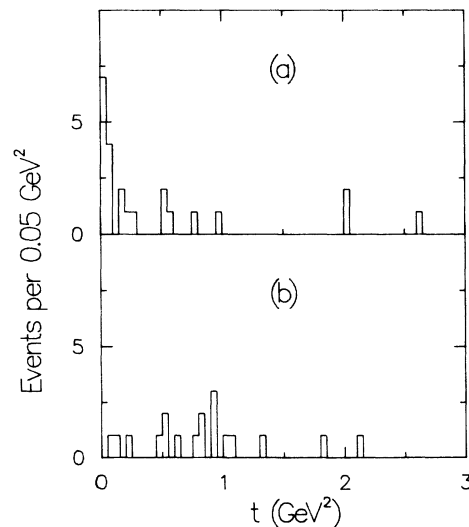


FIG. 4. t distribution for $\mu^-\rho^+$ events without (a) and with (b) identified protons.

of the target nucleons, and took account of our particular method of calculating t . Also, a neon-nucleus form-factor term was included, but Pauli exclusion principle effects were neglected.²⁴ The Monte Carlo model predicted that, for incoherent diffractive events, 21% would have $t < 0.1 \text{ GeV}^2$ and no visible recoil proton, while 77% would have either $t < 0.1 \text{ GeV}^2$ and a visible recoil proton or $t = 0.1 - 0.5 \text{ GeV}^2$. The observed 8 events in the latter category then imply 2.2 ± 0.8 events with $t < 0.1 \text{ GeV}^2$ and no visible proton. This second extreme leads to a ratio of all incoherent diffractive events to coherent events of 1.2 ± 0.6 , compared to the model prediction of 1.3 (assuming the same F_{abs} factor for both). The errors are large, but we see no order-of-magnitude discrepancy.

Finally, we take a background estimate, midway between the two extremes above, of 1.5 ± 1 events. Therefore, the net signal of coherent events at $t < 0.1 \text{ GeV}^2$ is 9.5 ± 3.5 events.

The distributions in visible hadron energy and in Q^2 are shown in Figs. 5 and 6 for the 11 events. Also in the figures are distributions for the 12 events with no protons and $t > 0.1 \text{ GeV}^2$ and for the 18 events with identified protons. Here, protons are not included in the hadron energy, and Q^2 is calculated assuming no missing neutral energy (since the neutrino energy is not known event by event). The figures show a qualitative difference between the 11 events and the other events, consistent with our interpreting them as from a different type of reaction. The low hadron energies in Figs. 5(b) and 5(c) are, of course, correlated with the low charged-particle multiplicity of these events.

We have checked for losses of coherent ρ events. One possible source of loss is via a truly primary γ being misassigned as a bremsstrahlung. (Note that the bremsstrahlung assignment algorithm contained no explicit reference to the relevant γ - γ mass.) So events with one primary γ plus one or more bremsstrahlung gammas (plus one positive hadron, no negative hadrons or vees, as above) were examined. One event was found for which, if one γ was reassigned from the bremsstrahlung to the primary category, the $m_{\gamma\gamma}$ and $m_{\pi^+\gamma\gamma}$ cuts above were satisfied and the calculated t value was $< 0.1 \text{ GeV}^2$. This event had no identified protons and was added to the coherent sample for all the following distributions [and is shown shaded in Figs. 5(a) and 6(a)].

A second possible (but not expected) loss is via a measurer failing to measure a primary γ . For a sample of Monte Carlo coherent ρ events, it was found that, if one γ was missed, 60% of the events would have a calculated t value $< 0.1 \text{ GeV}^2$. This percentage was essentially independent of neutrino energy, and agreed with the 54% obtained from the observed coherent events if one of their two gammas was randomly deleted. So the t distribution for events with just one primary γ (and one positive hadron, no negative hadrons or vees, as above) was examined. Eight events with no protons, and two events with protons, had $t < 0.1 \text{ GeV}^2$. Normalizing the background gave a net signal of 4.5 ± 3.5 events. In comparison, from the net two- γ signal plus our conversion, pointing, etc., efficiency plus the 0.60 fraction, we expect 5.5 coherent

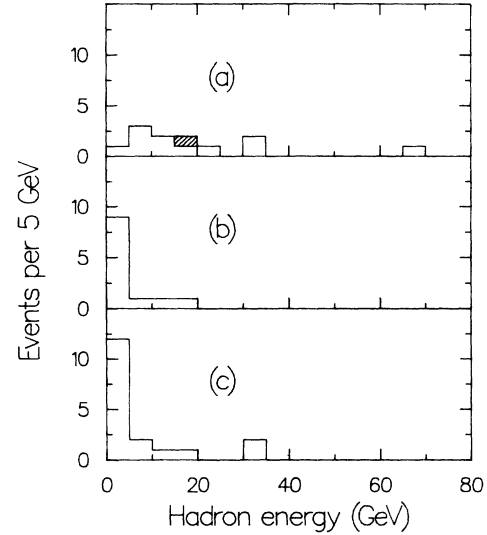


FIG. 5. Visible hadron energy for $\mu^- \rho^+$ events with (a) no protons and $t < 0.1 \text{ GeV}^2$, (b) no protons and $t > 0.1 \text{ GeV}^2$, and (c) protons (proton energy not included). Shaded event in (a) has a reassigned bremsstrahlung γ (see text).

one- γ events. We conclude that there is no evidence for any unexpected loss here.

COHERENT-EVENT RATE

To determine a rate for reaction (1), some corrections must be made: (a) the scanning efficiency for two-prong events with visible neutrals was 0.86, while the average efficiency for all charged-current events was 0.94; (b) the measuring, reconstructing, and pointing efficiency per γ was 0.90; (c) the probability that both gammas convert in the fiducial volume was 0.64; (d) the probability that the

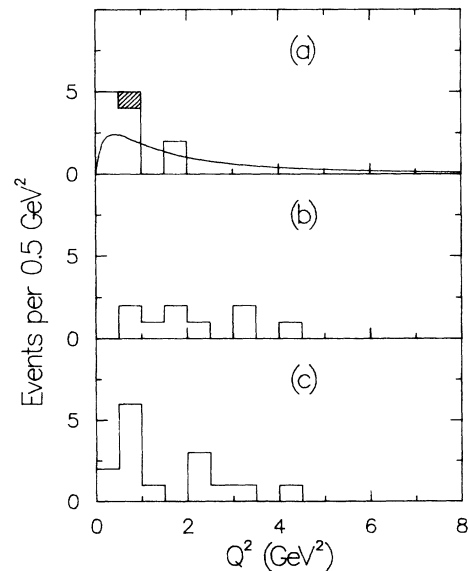


FIG. 6. Q^2 distribution for $\mu^- \rho^+$ events; (a)–(c) and shaded event as in Fig. 5. The curve in (a) is the theory prediction normalized to 12 events.

π^+ not interact before traveling far enough to pass the momentum error cut was 0.91; (e) the probability that true coherent events pass the $t < 0.1 \text{ GeV}^2$ cut (in spite of measurement errors) was 0.93. Then the 9.5-event net signal gives a rate, relative to all charged-current events, of $(0.28 \pm 0.10)\%$.

COMPARISON WITH THEORY

The above rate of $(0.28 \pm 0.10)\%$ can be compared with the prediction of the theory described above of 0.29%. This prediction is for our neutrino energy spectrum and takes into account the muon detection efficiency. Clearly these rates agree, although the errors are fairly large.

Table I gives the mean values of some kinematic quantities for the 12 events with $t < 0.1 \text{ GeV}^2$ and no protons. To calculate these quantities we assume that the events have no missing energy, as is appropriate if they are indeed coherent ρ meson events. Both the neutrino energy (Fig. 7) and Q^2 [Fig. 6(a)] distributions differ from the predictions. The median event energy for our neutrino beam is approximately 80 GeV; only 1 of the 12 events is above 80 GeV, whereas the prediction is that 54% will be above 80 GeV. Also, none of the events has $Q^2 > 2 \text{ GeV}^2$, whereas the predicted fraction above 2 GeV^2 is 42% (or 33% for events with neutrino energy $< 80 \text{ GeV}$).

The angular distributions for the ρ -meson decay for the 12 events are shown in Fig. 8. The ψ distribution has been folded appropriately so as to be in the range $0-\pi/2$. Mean values for the events and as predicted by the theory are given in Table II. In principle, these distributions provide information on the ratio R of the transverse and longitudinal parts of the cross section. The $\cos\theta$ and the ψ distributions do not agree well here; the former indicates $R \sim 1$, while the latter indicates $R \sim 0$. Taken together, they suggest an average R value of ~ 0.2 . This value gives a good fit to the angular distributions as shown in Fig. 8. We expect some Q^2 dependence to R , but the present statistics are too limited to investigate that.

It is interesting to look at comparisons of the diffractive vector-meson-dominance model with electroproduction and muoproduction experiments. A limitation is that the only relevant experiments used a hydrogen target. In an experiment with 11.5-GeV incident electrons,¹⁹ exclusive ρ -meson production data agreed with the model in the Q^2 dependence but not in the W (or, equivalently, ν) dependence. Two high-energy (in-

TABLE I. Mean values for some kinematical quantities. Data are the 12 $\mu^- \rho^+$ events with $t < 0.1 \text{ GeV}^2$ and no protons; theory is as described in text.

Variable	Data	Theory
E (GeV)	58 \pm 6	96
x	0.04 \pm 0.01	0.047
y	0.34 \pm 0.06	0.40
Q^2 (GeV^2)	0.73 \pm 0.15	2.74
ν (GeV)	20 \pm 5	36
E_μ (GeV)	38 \pm 5	59

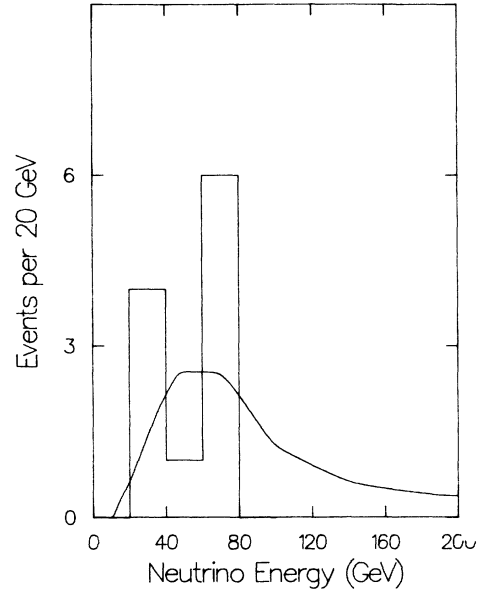


FIG. 7. Neutrino energy of 12 $\mu^- \rho^+$ events with no protons and $t < 0.1 \text{ GeV}^2$. The curve is the theory prediction normalized to 12 events.

cident muon energy $> 100 \text{ GeV}$) muoproduction experiments looking at exclusive ρ -meson data came to somewhat contradictory conclusions. One,²⁰ at $Q^2 < 2 \text{ GeV}^2$, found agreement with the model; the second,²⁵ at $1 < Q^2 < 15 \text{ GeV}^2$, found considerable disagreement. Part of the difficulty here lies in the data; in the region of Q^2 overlap of the two experiments, the cross sections do not disagree but the angular distributions apparently do.²⁶ Both experiments find a slope parameter (b in $\sigma \sim e^{-bt}$) that decreases in magnitude as Q^2 increases, suggesting

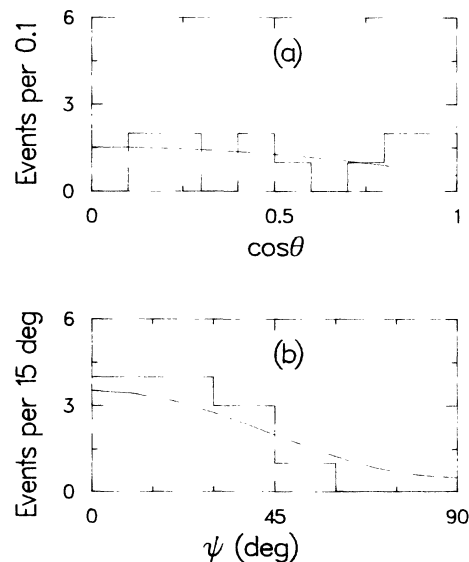


FIG. 8. (a) $\cos\theta$ and (b) ψ distributions of 12 events as in Fig. 7. θ is the ρ^+ -decay helicity polar angle. ψ is the difference of two azimuthal angles (see text) and has been folded to lie in the range $0-90$ deg. The curves superposed are predictions for $R = 0.2$ (see text).

TABLE II. Mean values for ρ -meson decay-angular distributions. The ψ distribution has been folded so as to lie in the range $0-\pi/2$. Data and theory as in Table I.

	Data	Theory, $R=0$	Theory, $R=1$
$ \cos\theta $	0.55 ± 0.08	0.37	0.55
ψ	0.40 ± 0.07	0.50	0.64

that a nondiffractive hard-scattering process becomes dominant, and hence that the diffractive process dies off at large Q^2 .

We conclude that the disagreement between our data and the model is not out of the line with the general trend of electroproduction and muoproduction experiments on a hydrogen target, although the situation there is somewhat unclear. On the other hand, in the coherent single-pion production by antineutrinos on neon,⁹ agreement is found with the analogous model, in particular on both Q^2 and incident-energy distributions, although the latter is almost all below 100 GeV and the former almost all below 2 GeV². In single-pion production, of course, the axial-vector rather than the vector component of the weak current is relevant.

CONCLUSIONS

In charged-current interactions of high-energy neutrinos in a neon-hydrogen bubble chamber, we have observed coherent ρ^+ production on neon nuclei. The net signal of 9.5 events gives a rate, relative to all charged-current events, of $(0.28\pm 0.10)\%$.

The overall rate agrees with the prediction of the vector-meson-dominance model. But at neutrino energies above 80 GeV the observed number of coherent events is significantly less than the predicted number. Also at Q^2 above 2 GeV² the observed number is less than that predicted.

ACKNOWLEDGMENTS

We are grateful to the Fermilab accelerator and 15-ft bubble-chamber staffs for the successful and productive run, and to our scanners and measurers for their careful work. We thank M. K. Gaillard for useful discussions. This work was supported in part by the U.S. Department of Energy and by the National Science Foundation. Part of the computing was supported by an IBM grant.

*Now at Medical Center, San Francisco, CA 94121.

†Now at Texas Accelerator Center, The Woodlands, TX 77380.

‡Now at Vista Research Inc., P.O. Box 51820, Palo Alto, CA 94303.

§Now at Arete Associates, P.O. Box 350, Encino, CA 91316.

**Now at Yale University, New Haven, CT 06511.

††Now at University of California, Riverside, CA 92521.

¹C. A. Piketty and P. Stodolsky, Nucl. Phys. **B15**, 571 (1970).

²M. K. Gaillard, S. A. Jackson, and D. V. Nanopoulos, Nucl. Phys. **B102**, 326 (1976); **B112**, 545(E) (1976).

³M. S. Chen, F. S. Henyey, and G. L. Kane, Nucl. Phys. **B118**, 345 (1977).

⁴M. K. Gaillard and C. A. Piketty, Phys. Lett. **68B**, 267 (1977).

⁵A. Bartl, H. Fraas, and W. Majerotto, Phys. Rev. D **16**, 2124 (1977).

⁶T. H. Bauer *et al.*, Rev. Mod. Phys. **50**, 261 (1978).

⁷E632 Collaboration, in *Neutrino '86: Neutrino Physics and Astrophysics*, proceedings of the 12th International Conference, Sendai, Japan, 1986, edited by T. Kitagaki and H. Yuta (World Scientific, Singapore, 1986), contributed paper No. 40.

⁸P. Marage *et al.*, Phys. Lett. **140B**, 137 (1984).

⁹P. Marage *et al.*, Z. Phys. C **31**, 191 (1986).

¹⁰WA59 Collaboration, P. Marage *et al.*, in *Neutrino '86: Neutrino Physics and Astrophysics* (Ref. 7), contributed paper No. 41.

¹¹H. J. Grabosch *et al.*, Z. Phys. C **31**, 203 (1986).

¹²H. C. Ballagh *et al.*, in *Neutrino '86: Neutrino Physics and As-*

trophysics (Ref. 7), p. 555.

¹³H. Faissner *et al.*, Phys. Lett. **125B**, 230 (1983).

¹⁴E. Ziskal, D. Rein, and J. G. Morfin, Phys. Rev. Lett. **52**, 1096 (1984).

¹⁵F. Bergsma *et al.*, Phys. Lett. **157B**, 469 (1985).

¹⁶C. Baltay *et al.*, Phys. Rev. Lett. **57**, 2629 (1986).

¹⁷Note that a factor of 2 error in the formula (and figures) of Ref. 3, and typographical errors in Refs. 2 and 3, make extraction of the correct formula from those two references somewhat difficult.

¹⁸D. Rein and L. M. Sehgal, Nucl. Phys. **B223**, 29 (1983).

¹⁹D. G. Cassel *et al.*, Phys. Rev. D **24**, 2787 (1981).

²⁰W. O. Shambroom *et al.*, Phys. Rev. D **26**, 1 (1982).

²¹P. Joos *et al.*, Nucl. Phys. **B113**, 53 (1976).

²²H. C. Ballagh *et al.*, Phys. Rev. D **21**, 569 (1980).

²³At small values of t , T_1/m_{Ne} is much smaller than unity, so that to a good approximation $t = p_1^2 + T_1^2$, as in Ref. 8.

²⁴R. J. Glauber, in *High Energy Physics and Nuclear Structure*, edited by S. Devons (Plenum, New York, 1970), p. 207.

²⁵J. J. Aubert *et al.*, Phys. Lett. **161B**, 203 (1985).

²⁶Note that in Fig. 4(b) of Ref. 25, which shows the relevant ρ decay matrix element for that experiment and for some electroproduction experiments, there are no points from Ref. 20. At least for $1 < Q^2 < 2$ GeV², values of the ratio R in Ref. 20 imply matrix-element values much closer to zero than those shown in the figure.